Assessing Potential Impacts of Offshore Wind Facilities on Regional Sea Scallop Laval and Early Juvenile Transports

PI: Changsheng Chen
Co-PIs: Liuzhi Zhao, Pingguo He, Robert C Beardsley, Kevin Stokesbury

SMAST-UMASSD

WOODS HOLE OCEANOGRAPHIC INSTITUTION 1930

NOAA Grant Number: NA19NMF450023

May 19, 2020

1.0 EXECUTIVE SUMMARY

Project Title: Assessing Potential Impacts of Offshore Wind Facilities on Regional Sea Scallop Laval and Early Juvenile Transports

Year Awarded: June 1, 2019-May 31, 2021

RSA Priorities Addressed By This Research: *GENERAL RESEARCH AREAS: Research to assess the impact of offshore wind energy development on the Atlantic sea scallop resource, including larval settlement and dispersal*.

A high-resolution, wind turbine-resolving coupled physical and scallop-IBM model is being developed under the platform of the Northeast Coastal Ocean Forecast System (NECOFS). This model is being applied to assess the potential impact of the offshore wind resource facilities on the regional fishery industry, especially on the connectivity between sea scallop populations of the Gulf of Maine/Georges Bank and Southern New England/Middle Atlantic Bight. This project is aimed at *a*) providing a scientific tool for the New England Fishery Management Council to assess potential impact of offshore wind facilities on the scallop larval transport/dispersion and the connectivity between the Gulf of Maine/Georges Bank and Middle Atlantic Bight; *b*) assessing the short-term (spawning period and early life stage each year) and long-term (inter-annual) impacts of the offshore wind turbines on regional sea scallop larvae transport, dispersion and connectivity through the direct comparisons between the cases with and without wind turbine installations; *c*) examining the sensitivity of the impact of offshore wind turbine development to climate-induced variability of scallop populations over the upstream sources; and *d*) evaluating an ongoing and proposed installation design of the offshore wind farm over the New England shelf to see if an optimal design could be proposed.

The BOEM approved the Vineyard Wind's site assessment plan (SAP) for the lease area of OCS-A-0501. Selecting this site, we successfully developed a high-resolution (up to ~1.0 m), wind-turbine-resolving subdomain FVCOM ocean model on the platform of NECOFS and coupled it with the regional Scallop-IBM model. A 39-year (1978-2016) Scallop-IBM model experiments were conducted to identify years which show the connectivity of sea scallop population between Georges Bank/Great South Channel and New England shelf as well as Mid-Atlantic Bight. The results indicate that the scallop larval settlement shows a significant interannual variability. We selected 2010 as a year for an initial assessment of the potential impact of the offshore wind developed in the Vineyard Wind's lease area of OCS-A-0501 on larval transport and found that during that year a large amount of larvae settled down near the lease area and also advected southward through Nantucket Shoal. Although Covid-19 Pandemic has significantly influenced our project, a high-resolution flow field with and without inclusion of wind turbines are being simulated. A scallop larval transport experiment will be carried out this summer.

Industry Partners: This project does not have a field component; therefore, no industry vessels have been involved in research. Six industry vessels from southern Massachusetts have started compensation fishing. They are "*Pamela Ann*, *Brittany Eryn*, *Madison Kate*, *Jane Elizabeth*, *Eileen Rita* and *Georges Banks*".

2.0 PRELIMINARY RESULTS AND DISCUSSION

- **Project goals and objectives**

The goal of this project is to assess the potential impact of the offshore wind facilities on the connectivity between sea scallop populations of the Gulf of Maine/Georges Bank and Southern New England/Middle Atlantic Bight. This overarching project goal is being achieved with objectives of:

1) coupling the scallop-IBM model with a high-resolution (up to ~1.0 m), wind turbine-resolving subdomain FVCOM ocean model under the framework of NECOFS;

2) identifying years which show the connectivity of sea scallop population between Georges Bank/Great South Channel and New England shelf as well as Mid-Atlantic Bight based on NECOFS-driven scallop-IBM model results and repeat the scallop-IBM experiments for those years under the 3-D physical fields from the high-resolution, wind turbine-resolving coupled subdomain-NECOFS system for the cases with and without inclusion of wind turbines;

3) conducting sensitivity analysis of larval transport/dispersion, subsequent recruitment and connectivity between regions (e.g., GB to MAB, northern MAB with southern MAB) to the offshore wind turbine development as spawning patterns/locations and intensities change on the upstream GB and GSC;

4) repeating the above experiments with different designs of offshore wind turbine development (e.g., cover area, locations and distance between turbine separation) and providing an optimal design with a balance between renewable energy development and commercial fisheries.

- **Development of a wind turbine resolving physical and Scallop-IBM model**

NS-FVCOM. The BOEM approved the Vineyard Wind's site assessment plan (SAP) for the lease area of OCS-A-0501. Vineyard Wind has proposed to install up to 100 wind turbine generators (WTGs) of 8 to 10 MW capacity in their lease area. Two alternative layouts (D1 and D2) are proposed with a separation spacing of ~0.75-1.0 nautical mile between individual WTGs (Fig. 1). In the D1 layout, WTGs will be aligned in a northwest-southeast orientation, whereas in the D2 layout, WTGs will be aligned in an east-west orientation. The towers of WTGs with capacity of 8 MV and 10 MV have diameters of approximately 20 feet (~6.1 m) and 28 feet (~8.5 m), respectively. Vineyard Wind proposed to mount individual WTG with either Monopile foundation or Jacket (Pin piles) foundation, with minimum and maximum foundation diameter sizes of 25 feet (~7.5 m) and 34 feet (~10.3 m) for Monopiles and 5 feet (~1.5 m) and 10 feet (~3.0 m) for Pin piles, respectively. Considering the construction influence area, we used the tower dimeter as the TWG's size to create the model grid for the case with TWGs in our previous BOEM-funded modeling work. Vineyard Wind's proposed TWG construction in the lease area of OCS-A-0501is significantly different from the TWGs configured in the present version of NS-FVCOM,

particularly in the total number of TWGs and the separation distance between individual TWGs.

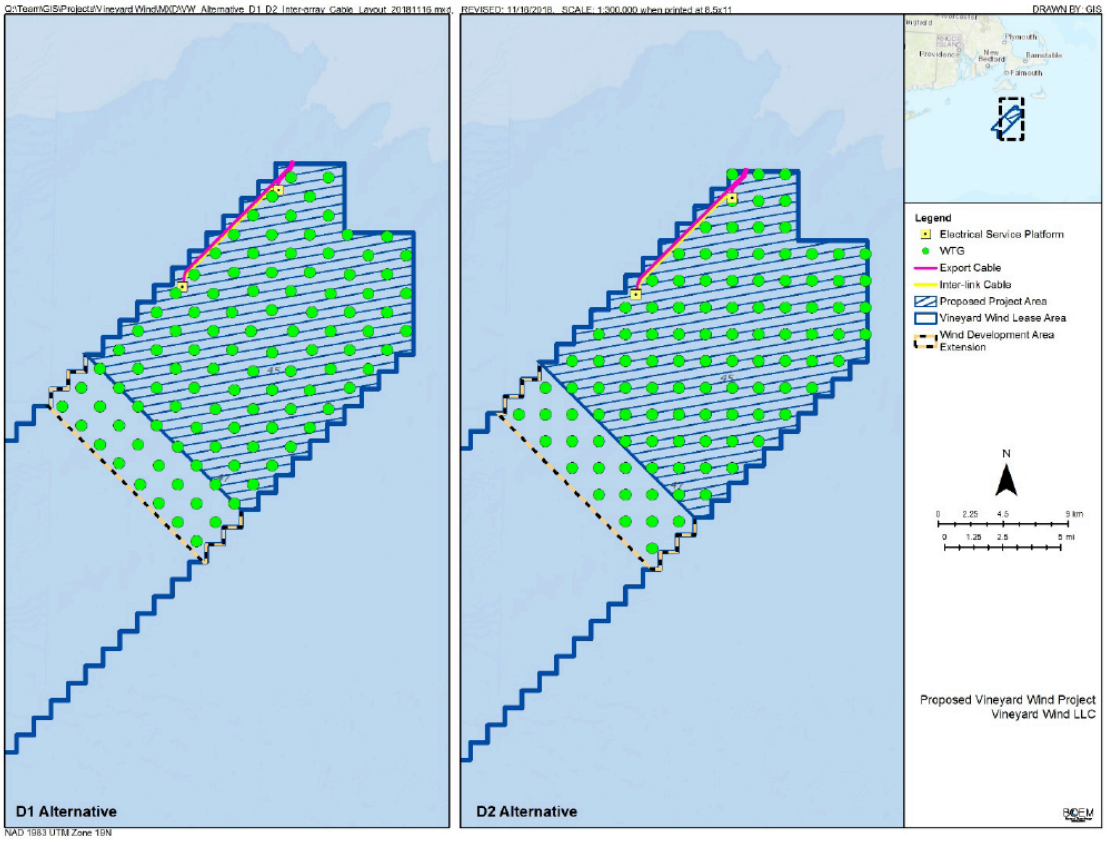

Fig. 1: Two alternative layouts (D1 and D2) of wind turbines proposed by Vineyard Wind LLC. D1: Align WTGs in a northwest-southeast orientation with a 1.0-nautical-mile spacing. D2: Align WTGs in an east-west orientation with 1.0-nautical mile spacing. This figure was a copy of Figure 2.1-5 in Vineyard Wind offshore wind energy project draft EIS (OCS EIS/EA, BOEM 2018-060).

We have developed the wind turbine-resolving model by modifying our existing wind turbine-resolving NS-FVCOM and NECOFS nested model system. We adjusted the number and locations of wind turbines in the NS-FVCOM domain to reflect the changes due to recent development of offshore wind energy facilities by leased companies. All the updated information about the layout design of offshore wind turbine constructions was from the Vineyard Wind's plan in the lease area of OCS-A-0501.

In our previous BOEM-funded modeling project (under contract No. M14PS00040), a total of 140 WTGs were configured in NS-FVCOM; 135 WTGs in the BOEM-issued lease areas in the MA and RI waters and 5 WTGs on the eastern shelf the Block Island. For each WTG, we considered a tower diameter of ~ 5 m (with a circumference of ~ 15.7 m). The separation spacing between individual WTGs was about ~5 km in the MA and RI waters and ~ 2.5 km around Block Island. The boundary of individual towers was constructed with about 12-13 triangular cells, which provided the reasonable resolving of the circular shape of a tower with a resolution of ~ 1.3 m around the circle boundary. The shortest side length of a triangular cell measured the resolution. The cell resolution changed from ~ 1.3 m to ~ 8 m over a distance of 10 m from the tower edge

and then to 200-300 m at the middle point between two towers.

For this project, we have used the same technology to re-configure 80-100 WTGs in the lease area of OCS-A-0501 by following Vineyard Wind proposed two alternative D1 and D2 layouts. When Task 1 was performed, we visited Vineyard Wind to inquire the updated design of the WTG construction and operation plan, and used the information to reconfigure the grid of NS-FVCOM. We have completed the reconfiguration of NS-FVCOM with options of D1 and D2 layouts. Figures 2 and 3 show the modified grids of NS-FVCOM based on Vineyard Wind D1 and D2 layouts. We have kept the horizontal resolution of ~1.0-1.3 m around the WTG tower. 11 σ-levels

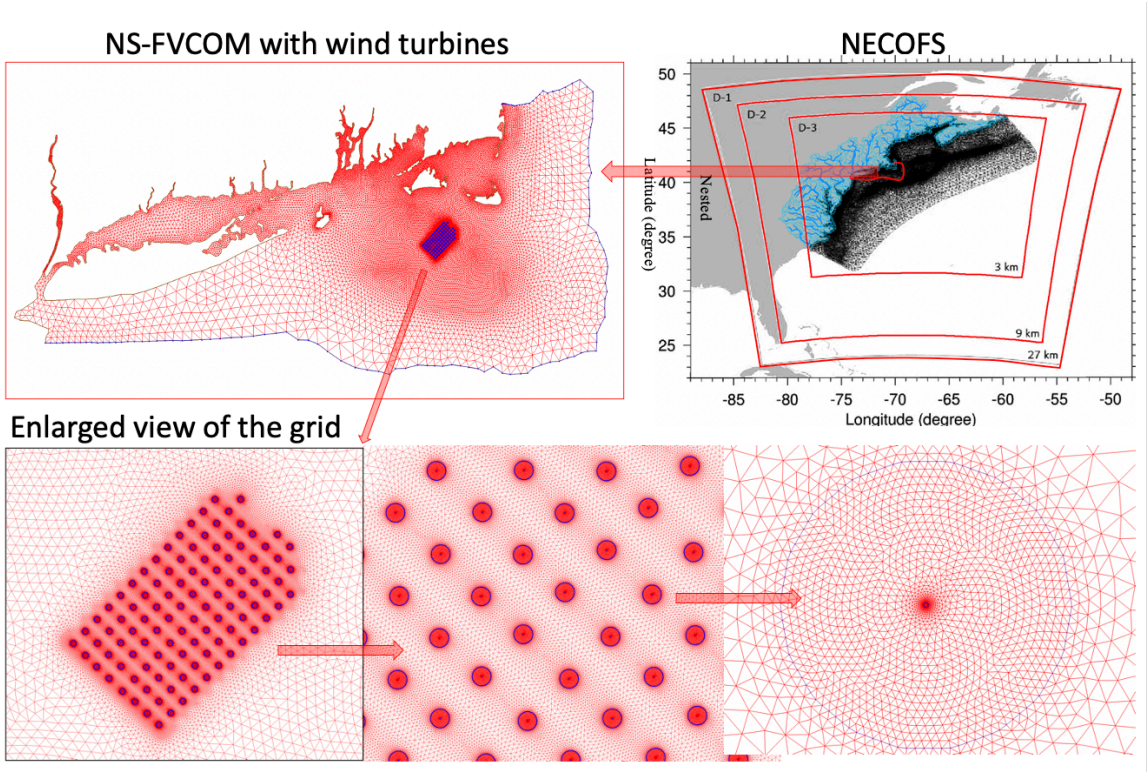

Fig. 2: The model grid of wind turbine-resolving NS-FVCOM for Vineyard Wind proposed D1 layout. A total of 106 wind turbine and supply facilities are included.

(10 layers) with a uniform thickness was specified in the vertical, which remains a vertical resolution of 4 m on the 40-m isobath and up to~0.5 m on the 5-m isobath. This vertical resolution is sufficient to resolve the vertical stratification in the lease area of OCS-A-0501 (Chen et al., 2016). An effort has been made on creating the efficiently performance grid with a shorter separation spacing of 0.75-1.0 nautical miles (1.39-1.85 km) between individual WTGs, which was about 1.4 to 2.7 times shorter than that configured in the previous version of NS-FVCOM used for BOEM project. For the modified NS-FVCOM, the total mesh and node numbers are 478,640 and 24,956 for D1 layout and 455,133 and 230,244 for D2 layout, respectively. Therefore, for the same horizontal resolution, the D2 layout requires less grids than the D1 layout.

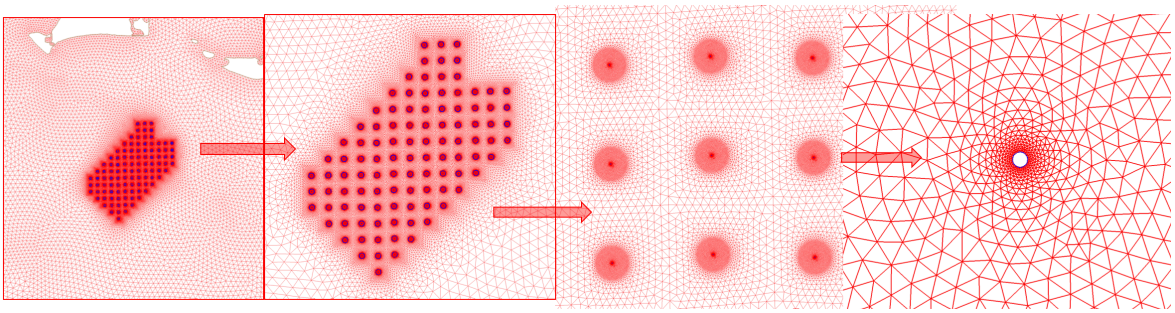

Fig. 3: The model grid of wind turbine-resolving NS-FVCOM for Vineyard Wind proposed D2 layout. A total of 106 wind turbine and suppl facilities are included.

The re-configured NS-FVCOM is a fully wave-current coupled hydrodynamic model that remains the same nesting boundary with GOM3-FVCOM (or updated version GOM5-FVCOM). For this project, we will run the model first without inclusion of current-wave interactions. This model will be driven by surface forcing (wind stress, surface heat flux plus short-wave irradiance, precipitation minus evaporation) with lateral boundary conditions specified through one-way nesting with GOM3-FVCOM. GOM3-FVCOM provides the initial and boundary conditions for hydrodynamics variables (the sea level, velocity, temperature, salinity, horizontal diffusion coefficient and vertical eddy viscosity). The surface forcing data are provided by the hindcast data-assimilated fields of the WRF model. WRF features the non-hydrostatic dynamics, terrain-following sigma-coordinate, variable domain and spatial resolution, multiple grid nesting, 4-D data assimilation, and several planetary boundary layer (PBL) modules to represent turbulent mixing over the ground and ocean (Grell, 1993). In NECOFS, the WRF model is configured with a "regional" domain (covering the Northeast U.S.) and a "local" domain (covering the Scotian Shelf/GOM/GB/NES) with horizontal grid spacing of 30 and 10 km, respectively. 31 non-uniform sigma levels were specified in the vertical, with a design to have finer resolution in the PBL. WRF uses the hydrostatic North American Mesoscale weather model fields as initial and boundary conditions. These two models were coupled through the two-way nesting approach. To improve the model based surface wind stress and heat flux estimates, we have implemented the COARE 3.0 bulk algorithm (Fairall et al., 1996, 2003) to NECOFS-WRF to re-calculate the air sea heat flux and wind stress. We have also integrated all coastal NDBC and C-MAN surface weather data in the local domain through 4-D data assimilation.

The nesting boundary of reconfigured NS-FVCOM consists of boundary cells with two boundary lines connected by triangle's nodes. FVCOM contains three types of one-way nesting boundaries: direct, indirect, and relaxed. In this contract work, we used the direct nesting method. Following this method, we first re-run the large domain GOM3-FVCOM, output all variables at nodes (surface elevation, temperature, salinity, vertical velocity) and cell centers (horizontal velocity) at every time step, and save these variables as a nesting boundary file. This nesting boundary file is then used to specify the hydrodynamic boundary condition for NS-FVCOM. It should be noted here that the surface elevation in the nesting boundary file contains both tidal and subtidal components.

Scallop-IBM. The IBM-based scallop population model consists of four pelagic phases (egg, trochophore, veliger, pediveliger (Figure 1). This model was significantly modified from the original version (Tian et al., 2009a), especially with inclusion of larval behavior in the surface mixed layer. Individual development in the model is based on age: eggs <2 days, trochophores 2–4 days, veligers 5–40 days, and pediveligers > 40 days (Stewart and Arnold, 1994). Behavioral vertical migration is specified for each life stage. Eggs are spawned on the seabed, are neutrally buoyant, and drift passively with vertical migration. Contrary to the existing models, trochophores have no directionality in their swimming and only randomly spin. Once the first shell is formed (prodisoconch) and the larvae form the 'D' configuration, then their center of gravity is below the velum, which propels them in the vertical direction upwards (Gallager, 1993; Gallager et al., 1996).

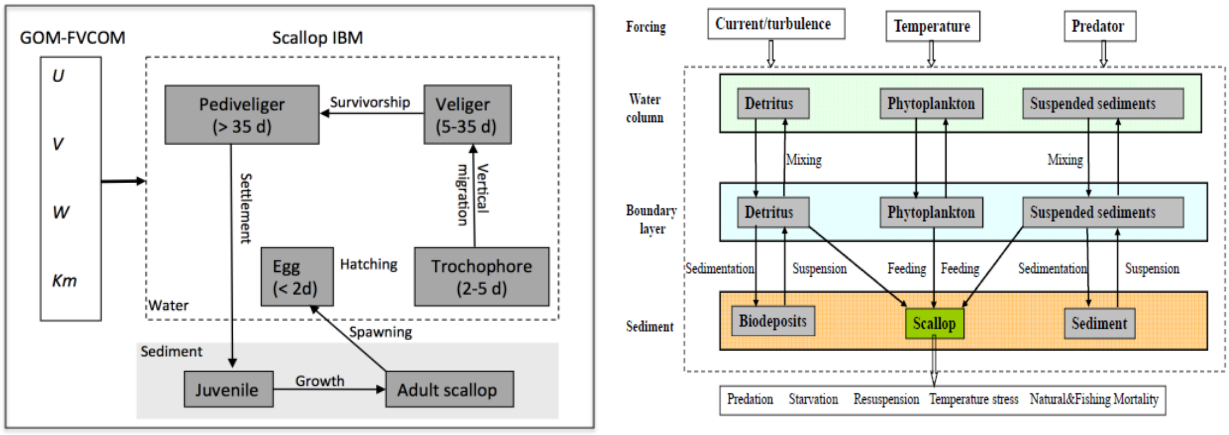

Fig.4: Structures of the scallop-IBM model. Upper: the scallop life stage model including 4 pelagic stages (egg, trochophore, veliger, and pediveliger) and 2 benthic stages (juvenile, and adult) Lower: details of the benthic stage model.

Veligers are essentially subject to current drift in the surface layers above the thermocline, but actively swim and alternately sink producing a distinct migration pattern. Veligers are sensitive to light transitions, *not* to any prolonged state of light intensity such as day or night (Gallager et al., 1996). Larvae between the ages of 5 and 45 days vertically migrate to the surface and then back to the thermocline both when the sun comes up and when it sets (Gallager et al., 1996). In addition, larvae respond to algal density (food) in a concentration-dependent way by spending more time at depths where algal density is higher (Gallager et al., 1996). Larvae also respond to ephemeral pulses of turbulence greater than 10^{-7} $W.Kg^{-1}$ by withdrawing their velum and sinking rapidly until the turbulent energy has subsided (Pearce et al., 1998). This extensive suite of swimming behaviors has never been captured in a model to date (e.g. Stewart and Arnold, 1994 and Tian et al., 2009a treated larvae as particles with a random walk) and could contribute greatly to the overall transport potential of larvae since they are constantly responding to stimuli and changing their depth. Late-stage pediveligers (>45 days) migrate downwards to the seabed (1.7 mm s^{-1}) to settle, but may remain at the thermocline for more than 100 days and delay metamorphosis if thermal conditions are inappropriate (Pearce et al., 1996). Such a delay in settlement could lead to higher retention if larvae are in a gyre that extends beyond the shelfbreak only to return several days later, particularly

in the MAB. Mortality throughout the pelagic phase can be carefully parameterized based on data and conditions provided in the literature (e.g. Gallager et al., 1986a,b, 1988).

A benthic stage with inclusion of feeding, predation, starvation, resuspension and natural/fishing mortality has been implemented into the current version of scallop-IBM. In the previous model, the sea scallop spat, juvenile and young adult are integrated into a single compartment "Scallop", but age, weight, and height attributes are simulated in a continuous manner. Age is incremented at each time step whereas shell height and weight are simulated based on trophodynamics and metabolism. Starvation mortality is linked to metabolism and food assimilation. Insufficient food assimilation to satisfy metabolism energy consumption results in starvation mortality (Ross and Nisbet, 1990). This happens when scallop larvae are dispersed and settled in regions where food items are scarce such as in the deep gulf and certain stratified regions over GB/GSC and MAB. Forcing includes current and turbulence diffusivity, temperature and predators. The NECOFS hourly archived currents and temperature will be used to drive the model and crab and starfish data will be used to specify predation pressure. Food items include phytoplankton, biogenic detritus and suspended terrestrial sediment, with each food compartment having different nutritional value parameterized as a growth efficiency coefficient. Suspended sediments do not possess any nutritional value, but they do interfere with the scallop filtration performance. The inclusion of this compartment is aimed at resolving the interference of suspended terrestrial detritus with the scallop food intake system and filtration clogging at high concentration of suspended matter. The phytoplankton and detritus field will be provided by the Nutrient-Phytoplankton-Zooplankton-Detritus (NPZD model simulation results.

- **Thirty-nine-year Scallop-IBM experiments**

We have conducted a set of scallop-IBM experiments to examining 1) how sensitive the scallop larval settlement is to the parameterization of scallop larval behavior in the early stages, 2) how the interannual variability of the subtidal circulation influence the scallop larval settlement in different years and 3) the connectivity of larval transport between GB, Great South Channel (GSC), Southern New England (SNE) and MAB region. Physical processes include the advection by flow field, water temperature, mixing intensity and mixed layer thickness. To qualify the role of physical processes, we first drive the IBM-based pelagic phase scallop population model by spawning based on multiyear averaged abundance and distribution of adult sea scallops for a 40-year period. The scallop data used to create the multiyear averaged field included video and HabCamV4 surveys from SMAST/UMASSD, NOAA and BIO/Canada. The SMAST data covers the period of 2003-2017, NOAA data covers the period of 1979-2017 (HabCam V4 survey) and BIO data covers the period of 2003-2017.

The results indicate that the scallop larval settlement exhibited a significant interannual variability, which was very sensitive to scallop larval behavior in their early stages. Taking the thermocline-seeking behavior into account increased the resident time of larvae in the water column over GB. As a result, the larvae, which were from eggs spawn on GB, mainly circulate with the clockwise residual flow around the bank and eventually settled on the bank, with only a few flowing southwards. This suggests that due to the lack of implementing the surface mixed layer dynamics in the scallop-IBM model, the connectivity of scallop larvae between GB and MAB were

significantly overestimated in previous works done by Tian et al. (2009). The larval transport to the MAB is closely related to the intensity of the cool pool and temperature front. The high abundance was found within the cool pool region over the SNE shelf and in the northern region of the MAB could be traced back to their origins in the closed area over the Nantucket Shoals close to the GSC.

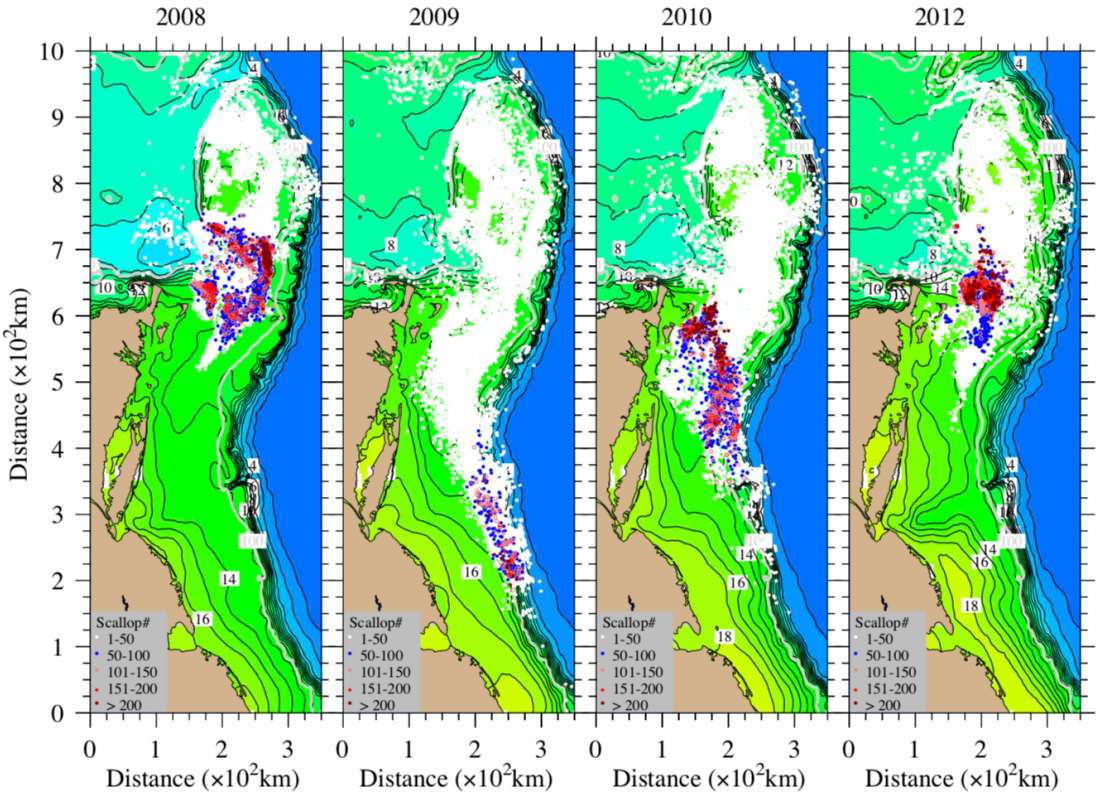

Fig.5: Settlement locations of super larval particles for 2008, 2009, 2010 and 2012 for the case with swimming in the mixed layer.

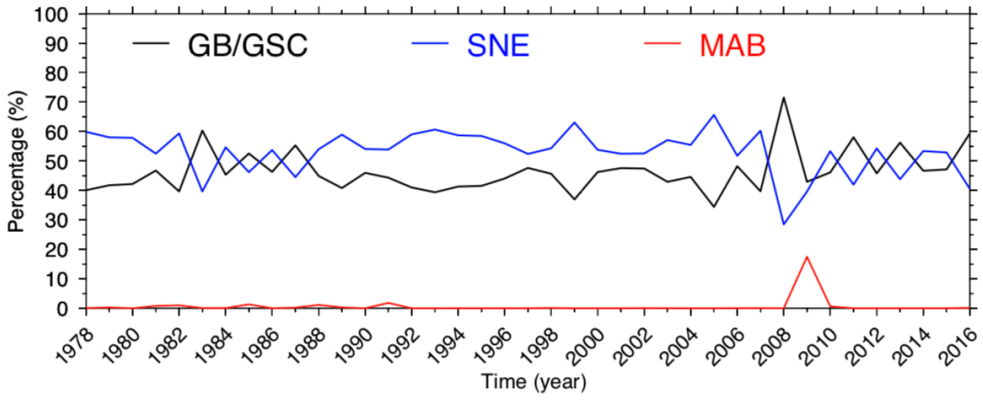

Fig. 6: Model-predicted percentages of the scallop larvae settling in the GB/GSC, SNE and MAB regions, respectively over the period of 1978-2016.

We also estimated the percentage of larvae settling over GB/GSC, SNE and MAB (Fig. 6). 2009 was a year which showed a significant southward larval transport from GB/GSC to SNE and MAB, while 2010 was a year with a large amount of larvae settling in the Vineyard Wind's leased area. Based on the 39-year simulation results, we decided 2009 and 2010 as years to examine how the development of the offshore wind in the Vineyard Wind's lease area affect the larval transport through that area.

3.0 SPECIAL COMMENTS

Due to Covid-19 Pandemic in the Massachusetts, the UMASSD has closed all laboratories since March, 2020. This has significantly influenced our project. Our high-performance cluster was shut down several times. In the past, the shutdown computer nodes can be easily turned on mutually by the computer manager, but now we have submitted a request to access the building, which usually took a few days for approval. For this reason, we have not been able to completed the high-resolution NS-FVCOM experiments for 2009 and 2010 yet.

We have completed the preparation of all forcing and boundary files to drive NS-FVCOM, and the model is being tested. We plan to complete the 2010 simulation in August and then 2009 simulation in the coming fall semester.

For the compensation fishing, COVID-19 has impacted our ability to complete the harvest of allocated RSA amount and the price of scallop harvested. There is a possibility that we may not be able to complete the allocated amount before the end of fishing year. We will have to request for “carryover” if this does occur.

4.0 REFERENCES

Chen, C., R. C. Beardsley, J. Qi and H. Lin, 2016. Use of Finite-Volume Modeling and the Northeast Coastal Ocean Forecast System in offshore wind energy resource planning. Final Report to the U.S. Department of the Interior, Bureau of Ocean Energy Management, Office of Renewable Energy Programs. BOEM 2016-050. 131pp.

Fairall, C. W., E. F. Bradley, D. P. Rogers, J. B. Edson, and G. S. Young, 1996: Bulk parameterization of air–sea fluxes for Tropical Ocean Global Atmosphere Coupled Ocean–Atmosphere Response Experiment, *Journal of Geophysical Research*, 101(C2), 3747–3764.

Fairall, C. W., E. F. Bradley, J. E. Hare, A. A. Grachev, and J. B. Edson, 2003. Bulk parameterization of air-sea fluxes: updates and verification for the COARE algorithm, *J. Climate*, 16, 571-591, doi: 10.1175/1520-0442(2003)016.

Gallager, S. M., and R. Mann, 1986a. Growth and survival of larvae of *Mercenaria mercenaria* (L.) *Crassostrea virginica* (Gmelin) and *Placopecten magellanicus* relative to lipid content of eggs and broodstock conditioning. *Aquaculture,* 56(2): 105-121.

Gallager, S. M., R. Mann, and G. L. Sasaki, 1986b. Lipid as an index of growth and viability in three species of bivalve larvae. *Aquaculture,* 56(2), 81-103.

Gallager, S. M., 1988. Visual observations of particle manipulation during feeding in larvae of bivalve molluscs. *Bull. Mar. Sci.,* 43(3), 344-365.

Gallager, S. M., 1993. Hydrodynamic disturbances produced by small zooplankton: a case study for veliger larvae of bivalve molluscs. *J. Plankton Res*., 15(11), 1277-1296..

Gallager, S. M., J. L. Manuel, D. A. Manning and R. O'Dor, 1996. Ontogenetic changes in the vertical distribution of scallop larvae *Placopecten megellanicus* in 9 m-deep mesocosms as a function of light, food, and temperature stratification. *Mar. Biol.,* 124, 679-692.

Grell, G. A., 1993: Prognostic evaluation of assumptions used by cumulus parameterizations, *Mon. Wea. Rev*., 121, 764–787.

OCS EIS/EA, BOEM2018-060: Vineyard Wind offshore wind energy project draft environmental impact statement, December 2018, U.S. Department of the Interior, Bureau of Ocean Energy Management, 478pp.

Pearce, C. M., R. K. O'Dor, S. M. Gallager, D. A. Manning and E. Bourget, 1996. Settlement of sea scallop *Placopecten magellanicus* larvae in 9 m deep mesocosms as a function of food distribution, thermoclines, depth, and substratum. *Mar. Biol.,* 124(4), 693-706.

Pearce, C. M., S. M. Gallager, D. A. Manning, R. K. O'Dor and E. Bourget, 1998. Effect of thermoclines and turbulence on depth of larval settlement and spat recruitment of the giant scallop Placopecten magellanicus larvae in 9 m-deep laboratory mesocosms. Mar. Ecol. Progr. Ser., 165, 195-215.

Stewart, P. L. and S. H. Arnold, 1994. Environmental requirements of the sea scallop (Placopectenmagellanicus) in eastern Canada and its response to human impacts. Can. Tech Rep. Fish. Aquat. Sci. 2005, 1– 36.

Tian, R. C., C. Chen, K. D. E. Stokesbury, B. J. Rothschild, Q. Xu, G. W. Cowles, B. P. Harris and M. C. Marino II, 2009. Sensitivity analysis of sea scallop (Placopectenmagellanicus) larvae trajectories to hydrodynamic model configuration on Georges Bank and adjacent coastal regions. Fish. Oceanogr., 18, 173-184.